Prediction of Progression-free Survival for Stage IB-IIA Non-small Cell Lung Cancer Based on CT Morphological Features and Clinicopathological Characteristics

Junjun Liang[1*], Yunjin Long[2], Haotian Zhu[3], Xin Yang[2], Huanlong Lu[4], Xun Wang[5]

[1] Guangzhou First People's Hospital, Guangzhou 510030, China

[2] Zunyi Medical University, Zunyi 563000, China

[3] South China University of Technology, Guangzhou 511400, China

[4] Qiannan People's Hospital, Duyun 558000, China

[5] Shanghai Jiao Tong University School of Medicine Affiliated Ninth People's Hospital, Shanghai 200000, China

[*] Corresponding author: Junjun Liang, Department of Radiology, Guangzhou First People's Hospital, Guangzhou 510030, China; E-mail: 1550625590@qq.com

DOI: 10.32629/jcmr.v5i4.3035

Abstract: Objectives: The aim of this study is to evaluate the feasibility of computed tomography (CT) morphological features and clinicopathological characteristics in predicting progression-free survival (PFS) for patients with stage IB-IIA non-small cell lung cancer (NSCLC). Methods: A total of 95 patients with stage IB-IIA NSCLC who underwent CT scans and surgical resection were retrospectively included in our study. The CT morphological features and clinicopathological characteristics were assessed by two observers. Univariate and multivariate cox proportional hazards regression analysis were used to identify significant PFS predictors and construct prediction model. The area under the receiver operating characteristic (ROC) curve (AUC) was used to evaluate the predictive ability of the model for progression-free survival at 1-, 2- and 3-years. In internal validation, the predictive model was subjected to bootstrapping validation (1000 bootstrap resamples) to calculate the overall relative C-index. Results: Progression were found in 17 patients (17.9%, 17/95). Four risk factors were determined in the multiple stepwise Cox regression analysis, including male, age, sublobectomy, and lobulation, as well as CT diameter. The AUC of the model for predicting 1, 2, and 3 years PFS was 0.899, 0.799 and 0.833, respectively. In the internal validation cohort, the overall relative C index of the model was 0.82. The model showed good prediction performance. Conclusion: The model constructed from CT morphological features and clinicopathological characteristics helps predict PFS in patients with stage IB-IIA NSCLC and distinguish between high-risk and low-risk patients, which could help the doctor make Postoperative decisions.

***Keywords*:** non-small cell lung cancer; progression-free survival; computed tomography

1. Introduction

Lung cancer is one of the most prevalent malignancies worldwide, with high incidence and mortality rates[1, 2, 3]. Among these, early-stage NSCLC, which mainly includes lesions limited to stages IA, IB, and IIA, exhibits a significantly better prognosis compared to advanced NSCLC. Early-stage NSCLC is primarily treated with surgical resection[4]. The prognosis for patients with stage IB-IIA NSCLC varies significantly, and some may experience postoperative recurrence or death. There is an urgent need to establish a more reliable prognostic prediction model to predict the postoperative prognostic risk of stage IB-IIA NSCLC and guide the personalized treatment plan after surgery.

CT is a cornerstone in the diagnosis, treatment planning, and follow-up of Non-Small Cell Lung Cancer (NSCLC). CT morphological features are assessed by radiologists in a straightforward manner. Researchers[5, 6] have utilized CT subjective features and clinical information to construct preoperative prediction models for predicting adverse prognostic factors, such as pleural invasion and occult lymph node metastasis in NSCLC, thereby CT morphological features may also significantly influence the prognosis of non-small cell lung cancer. However, to the best of our knowledge, there is a scarcity of studies focusing on predicting the postoperative prognosis of stage IB-IIA NSCLC based on CT morphological features. Given this context, this study aims to explore the potential of combining CT morphological features inside and outside the tumor to develop a progression-free survival prediction model for stage IB-IIA NSCLC, distinguishing between high-risk and low-risk patients, and thereby providing personalized treatment decision support for clinical practice.

2. Methods

2.1 Patients

This study received study-specific institutional review board approval and obtained a waiver of informed consent. A total of 95 patients between February 2017 and August 2021, with surgically confirmed stage IB-IIA non-small cell lung cancer (NSCLC) and who underwent a CT scan within 2 weeks of surgical resection, were retrospectively enrolled. The patient selection process is illustrated in Figure 1. The primary endpoint of the study was progression-free survival (PFS), defined as the time from the date of surgery to the date of recurrence or death. Follow-up was completed in September 2023.

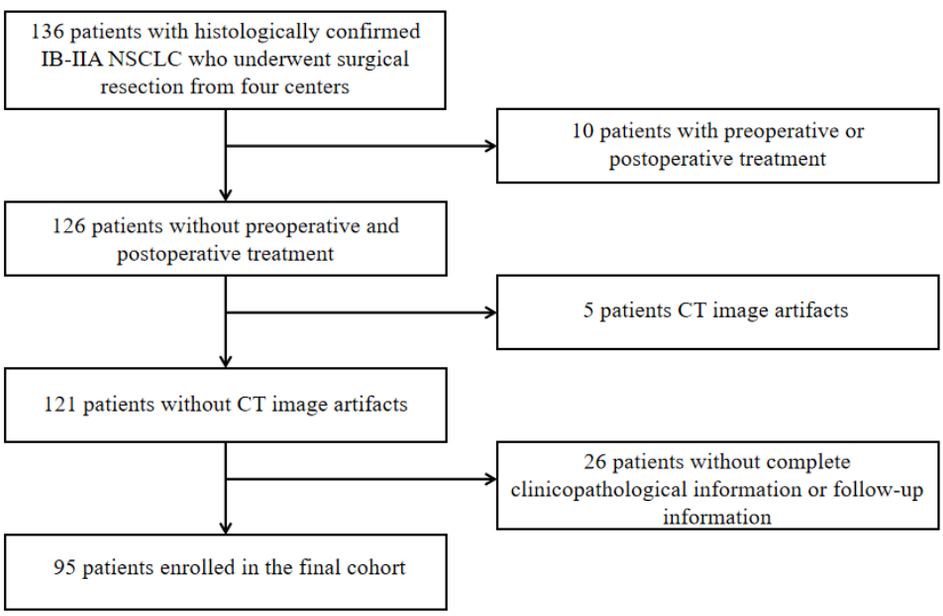

Figure 1. Flowchart showing the selection of patients with stage IB-IIA NSCLC

2.2 CT image acquisition

All patients were scanned using imaging devices of GE 64-slice VCT or Somatom Definition Flash. The scanning parameters were 120 kVp with the automatic regulation of the tube current and a reconstruction thickness of 0.5-2 mm. After acquiring unenhanced images, all patients were injected with intravenous nonionic iodinated contrast agents. The images of the arterial and venous phases were collected at 25 and 60 seconds after the injection of contrast agents, respectively.

2.3 Image features

Two radiologists with 7 and 5 years of experience in chest imaging diagnosis, respectively, independently assessed the CT morphological features. Both were blinded to clinical and pathological data. Disagreements between the two radiologists were resolved by a third radiologist with 15 years of experience in chest imaging. The CT morphological features evaluated included: location side, location lobe, CT diameter, CT solid part diameter, texture, lobulation, spiculation, calcification, air bronchogram, bubblelike lucency, cavity, pleural attachment, pleural retraction, bronchovascular bundle thickening, clinically positive lymph nodes, obstructive pneumonia and peripheral emphysema, peripheral fibrosis.

2.4 Statistical Analysis

All statistical analyses were conducted using R version 4.0.5 and SPSS version 26.0. The agreement between the two radiologists was assessed using Cohen's Kappa coefficient or the intra-class correlation coefficient (ICC). Continuous variables were reported as means with standard deviations (SD) or medians with interquartile ranges (IQR), as appropriate. Categorical variables were presented as counts and percentages. For continuous variables, a paired t-test or the Mann-Whitney U test was employed, and for categorical variables, the chi-square test was used. Cox proportional hazards regression models were utilized to calculate hazard ratios (HR), and Kaplan-Meier survival curves were plotted. AUC was employed to evaluate the predictive power of the model for progression-free survival at 1, 2, and 3 years. In internal validation, the predictive model was subjected to bootstrapping validation (1000 bootstrap resamples) to calculate the overall relative C-index. $P < 0.15$ in the Univariate Cox regression analysis was considered statistically significant, while all other $P < 0.05$ were considered statistically significant.

3. Results

3.1 Patient demographics and CT image features

A total of 95 eligible patients were enrolled in our study. The consistency of CT image feature evaluation by the two radiologists was good, with Cohen's Kappa and ICC values all exceeding 0.80. Table 1 summarizes the clinicopathological characteristics and CT morphological features of the patients. No significant differences were observed in all clinicopathological factors and CT image features between the Non-Progression and Progression groups, except for gender (P = 0.047) , age (P = 0.046) , CT diameter (and P = 0.045) and peripheral emphysema (P = 0.017).

Table 1. CT morphological features and clinicopathological characteristics in the non-progression group and progression group of patients with stage IB-IIA NSCLC

Characteristic	Total(n=95)	Non-Progression(n=78)	Progression(n=17)	P
Gender, n (%)				
Female	37(38.9)	34(43.6)	3(17.6)	0.047
Male	58(61.1)	44(56.4)	14(82.4)	
Age(year)	63 ± 9.8	64(55, 70)	68 ± 7.5	0.046
Smoking history, n (%)				
No	63(66.3)	54(69.2)	9(52.9)	0.198
Yes	32(33.7)	24(30.8)	8(47.1)	
pT stage, n (%)				
T2a	83(87.4)	68(87.2)	15(88.2)	1.000
T2b	12(12.6)	10(12.8)	2(11.8)	
Histological type, n (%)				
Adenocarcinoma	69(72.6)	60(76.9)	9(53.0)	
Squamous cell	14(14.7)	10(12.8)	4(23.5)	0.131
Adenosquamous cell	3(3.1)	2(2.6)	1(5.9)	
Other	9(9.5)	6(7.7)	3(17.6)	
Visceral pleural invasion, n (%)				
No	27(28.4)	24(30.8)	3(17.6)	0.429
Yes	68()	54(69.2)	14(82.4)	
Vascular_invasion, n (%)				
No	82(86.3)	70(89.7)	12(70.6)	0.090
Yes	13(13.7)	8(10.3)	5(29.3)	
Operation, n (%)				
Lobectomy	79(83.2)	68(87.2)	11(64.7)	0.059
sublobectomy	16(16.8)	10(12.8)	6(35.3)	
Pathological tumor diameter (cm)	3.0(1.8, 4.0)	2.5(1.8, 4.0)	3.3 ± 0.9	0.110
Location side, n (%)				
Left	41(43.2)	31(39.7)	10(58.9)	0.150
Right	54(56.8)	47(60.3)	7(41.1)	
Location lobe, n (%)				
upper lobe	59(62.1)	46(59.0)	13(76.5)	0.178
Middle or Lower lobe	36(37.9)	32(41.0)	4(24.5)	
CT diameter (cm)	2.8(1.8, 3.8)	2.7(1.7, 3.7)	3.3(2.6, 4.1)	0.045
CT solid part diameter (cm)	2.1(1.4, 3.5)	2(1.3, 3.4)	3.2 ± 1.9	0.065
Texture, n (%)				
pure GGO*	5(5.3)	4(5.1)	1(5.9)	
Mixed GGO with solid part <50%	10(10.5)	9(11.5)	1(5.9)	0.836
Mixed GGO with solid part > 50%	17(17.9)	15(19.2)	2(11.7)	
Solid	63(66.3)	50(64.2)	13(76.5)	

Lobulation, n (%)				
No	12(12.6)	8(10.2)	4(23.5)	0.276
Yes	83(87.4)	70(89.8)	13(76.5)	
Spiculation, n (%)				
No	26(27.4)	22(28.2)	4(23.5)	0.927
Yes	69(72.6)	56(71.8)	13(76.5)	
Calcification, n (%)				
No	90(94.7)	74(94.9)	16(94.1)	1.000
Yes	5(5.3)	4(5.1)	1(5.9)	
Air bronchogram, n (%)				
No	54(56.8)	43(55.1)	11(64.7)	0.470
Yes	41(43.2)	35(44.9)	6(35.3)	
Bubblelike lucency, n (%)				
No	71(74.7)	57(73.1)	14(82.4)	0.624
Yes	24(25.3)	21(26.9)	3(17.6)	
Cavity, n (%)				
No	82(86.3)	69(88.5)	13(76.5)	0.361
Yes	13(13.6)	9(11.5)	4(23.5)	
Pleural attachment, n (%)				
No	36(37.9)	30(38.5)	6(35.3)	0.807
Yes	59(62.1)	48(61.5)	11(64.7)	
Pleural retraction, n (%)				
No	27(28.4)	24(30.8)	3(17.6)	0.429
Yes	68(71.6)	54(69.2)	14(82.4)	
Bronchovascular bundle thickening, n (%)				
No	39(41.1)	31(39.7)	8(47.1)	0.579
Yes	56(58.9)	47(60.3)	9(53.0)	
Clinically positive lymph nodes, n (%)				
No	79(83.2)	68(87.2)	11(64.7)	0.059
Yes	16(16.8)	10(12.8)	6(35.3)	
Obstructive pneumonia, n (%)				
No	86(90.5)	70(89.7)	16(94.1)	0.920
Yes	9(9.5)	8(10.3)	1(5.9)	
Peripheral emphysema, n (%)				
Absence	74(77.9)	65(83.3)	9(53.0)	0.017
Slight or Moderate	18(18.9)	11(14.1)	7(41.1)	
severe	3(3.2)	2(2.6)	1(5.9)	
Peripheral fibrosis, n (%)				
No	88(92.6)	74(94.9)	14(82.4)	0.201
Yes	7(7.4)	4(5.1)	3(17.6)	

* ground-glass opacity.

3.2 Follow-up and recurrence

The mean follow-up time for the study sample was 42.9±20.4 months. During this period, 17 patients (17.9%, 17/95) experienced recurrence or death, with a median progression-free survival (PFS) of 15.4 (6.5, 23.1) months.

3.3 Predictive model construction and validation for progression-free survival

In univariate Cox regression analysis, 11 related factors were screened ($P < 0.15$), and then 4 factors were finally selected by multivariate Cox stepwise regression analysis, including male, age, sublobectomy, lobulation, and CT diameter(Table 2), and a prediction model constructed by them. The AUC of the model for predicting 1-, 2-, and 3-year progression-free sur-

vival was 0.899, 0.799, and 0.833, respectively(Figure 2). According to the optimal cut-off value of the model, the patients were divided into high-risk and low-risk cohorts, and the KM survival curve analysis demonstrated a significant statistical difference between the high-risk and low-risk groups ($P < 0.001$), as shown in Figure 3. The comprehensive prediction model could effectively distinguish patients at high risk of progression from those at low risk. In the internal validation cohort, the overall relative C-index of the model was 0.82. Overall, the model exhibited good predictive performance.

Table 2. Univariate and multivariate cox regression analyses of CT morphological features and clinicopathological characteristics in predicting PFS of stage IB-IIA NSCLC

Characteristic	Univariable analysis HR [95% CI]	P	Multivariable analysis HR [95% CI]	P
Gender				
Female	Ref		Ref	
Male	3.33(0.96-11.59)	0.059	5.25(1.35-20.41)	0.017
Age(year)	1.06(1.01-1.12)	0.029	1.06(1.00-1.12)	0.045
Smoking history				
No	Ref			
Yes	1.95(0.20-3.89)	0.168		
pT stage				
T2a	Ref			
T2b	0.89(0.38-14.31)	0.875		
Histological type				
Adenocarcinoma	Ref			
Squamous cell	2.64(0.81-8.60)	0.107		
Adenosquamous cell	2.75(0.35-21.74)	0.339		
Other	2.88(0.78-10.66)	0.114		
Pleural invasion				
No	Ref			
Yes	2.27(1.07-8.70)	0.207		
Vascular_invasion				
No	Ref			
Yes	3.06(0.33-4.85)	0.036		
Operation				
Lobectomy	Ref			
sublobectomy	3.40(1.25-9.22)	0.016	3.75(1.18-11.89)	0.025
Pathological diameter	1.3(0.88-1.9)	0.182		
Location side				
Left	Ref			
Right	0.49(0.19-1.29)	0.149		
Location lobe				
upper lobe	Ref			
Middle or Lower lobe	0.47(0.15-1.44)	0.185		
CT diameter	1.33(1.00-1.78)	0.052	1.45(1.06-2.00)	0.021
CT solid part diameter	1.28(0.99-1.67)	0.063		
Texture				
pure GGO*	Ref			
Mixed GGO with solid part <50%	0.48(0.03-7.75)	0.608		
Mixed GGO with solid part > 50%	0.53(0.05-5.88)	0.606		
Solid	1.11(0.14 - 8.47)	0.922		
Lobulation				
No	Ref			
Yes	0.42(0.14 - 1.29)	0.128	0.13(0.04-0.51)	0.003

Spiculation				
No	Ref			
Yes	1.17(0.38-3.60)	0.781		
Calcification				
No	Ref			
Yes	1.07(0.14-8.10)	0.95		
Air bronchogram				
No	Ref			
Yes	0.65(0.24-1.75)	0.39		
Bubblelike lucency				
No	Ref			
Yes	0.62(0.18-2.15)	0.448		
No	Ref			
Yes	2.23(0.73-6.86)	0.161		
Pleural attachment				
No	Ref			
Yes	1.06(0.39-2.88)	0.909		
Pleural retraction				
No	Ref			
Yes	1.90(0.55-6.62)	0.312		
Bronchovascular bundle thickening				
No	Ref			
Yes	0.77(0.30- 2.00)	0.595		
Clinically positive lymph nodes				
No	Ref			
Yes	3.44(1.27 - 9.33)	0.015		
Obstructive pneumonia				
No	Ref			
Yes	0.53(0.07-4.01)	0.539		
Peripheral emphysema				
Absence	Ref			
Slight or Moderate	4.33(1.61-11.66)	0.004		
severe	4.03(0.51-32.0)	0.188		
Peripheral fibrosis				
No	Ref			
Yes	4.09(1.16-14.42)	0.028		

* ground-glass opacity.

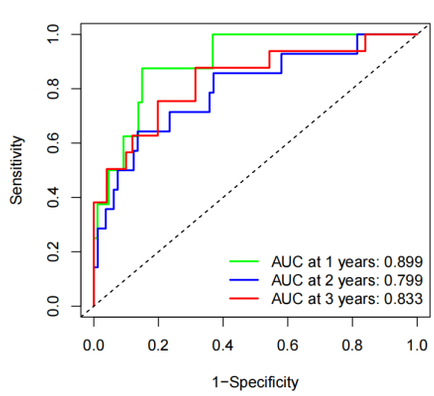

Figure 2. The ROC curves of model for predicting 1-, 2-, and 3-years progression-free survival

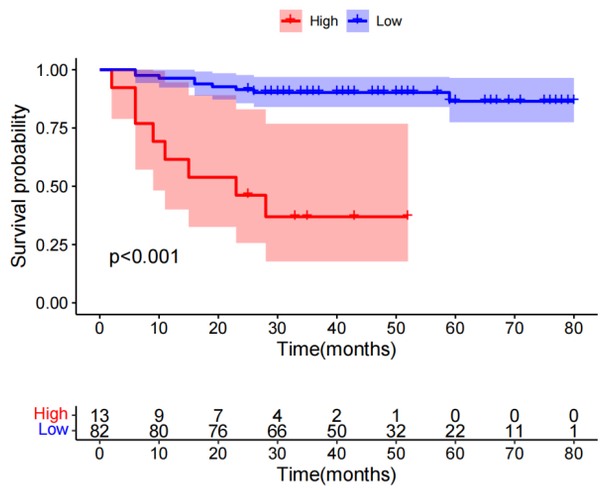

Figure 3. KM survival curve of high-risk cohort and low-risk cohort

4. Discussion

With the advancement of medical imaging technology, patients with early-stage NSCLC now have the opportunity to be diagnosed and treated early. CT is a commonly utilized tool for the diagnosis, treatment guidance, and follow-up of NSCLC. Despite early treatment, some patients may still experience disease progression, which significantly impacts their survival and quality of life. For stage IB-IIA NSCLC, the accurate identification of high-risk patients and the administration of postoperative adjuvant therapy are crucial for enhancing the postoperative quality of life of patients.

CT morphological features are subjectively evaluated by radiologists and are intuitive and interpretable. Sun et.al[6] have predicted visceral pleural invasion in pleural-based lung cancer subtypes, utilizing a variety of CT morphological features. The AUC values for pleural label type and pleural contact type NSCLC were 0.84 and 0.78, respectively, indicating good predictive power, Zhao et.al[5] discovered that the prediction model for occult lymph node metastasis in stage IA-IIA NSCLC, which was developed by integrating CT morphological features such as the diameter of the solid part of the tumor, bronchovascular bundle thickening, lobulation, and obstructive pneumonia, exhibited high predictive accuracy. The model's AUC values were 0.821 and 0.788 in the training and validation sets, respectively. To the best of our knowledge, there are limited studies that have utilized CT morphological features to predict PFS in patients with stage IB-IIA NSCLC. To date, while some scholars have attempted to predict the prognosis of NSCLC based on conventional clinicopathological factors or molecular markers alone, their predictive accuracy remains suboptimal[7-12]. In this study, we analyzed 18 CT morphological features and 9 clinical case features. Our findings indicated that older age and male were significantly associated with disease progression, that is consistent with the findings of the study by Zeng et al[13]. Our study further revealed that sublobectomy is a significant factor in disease progression. Sublobectomy is a surgical procedure that is restricted in its scope. Consequently, patients may face a heightened risk of disease progression if surgery fails to sufficiently remove potential micrometastases surrounding the tumor[14]. Zheng et.al[15] found that the CT diameter is a significant predictor of poor prognosis, a finding consistent with our study. This may be attributed to the fact that a larger diameter of malignant tumor indicates greater pathological invasion and a more aggressive tumor behavior, leading to a poorer prognosis[16, 17].

This study is subject to several limitations. Firstly, it is a retrospective analysis, which may introduce bias and limit the generalizability of the findings. Secondly, external validation of the model's accuracy is lacking. For future research, it is imperative to prospectively collect data in a true external setting to validate the current study's results.

5. Conclusion

In conclusion, the prediction model, which utilizes CT morphological features and clinicopathological factors, is capable of predicting PFS in patients with stage IB-IIA NSCLC and effectively distinguish between high-risk and low-risk patients, thereby aiding in clinical treatment decision-making.

References

[1] SUNG H, FERLAY J, SIEGEL R L, et al. Global Cancer Statistics 2020: GLOBOCAN Estimates of Incidence and

Mortality Worldwide for 36 Cancers in 185 Countries [J]. CA Cancer J Clin, 2021, 71(3): 209-249.
[2] SIEGEL R L, MILLER K D, WAGLE N S, et al. Cancer statistics, 2023 [J]. CA Cancer J Clin, 2023, 73(1): 17-48.
[3] SIEGEL R L, MILLER K D, FUCHS H E, et al. Cancer Statistics, 2021 [J]. CA Cancer J Clin, 2021, 71(1): 7-33.
[4] ETTINGER D S, WOOD D E, AISNER D L, et al. NCCN Guidelines Insights: Non-Small Cell Lung Cancer, Version 2.2021 [J]. J Natl Compr Canc Netw, 2021, 19(3): 254-266.
[5] ZHAO F, ZHAO Y, ZHANG Y, et al. Predictability and Utility of Contrast-Enhanced CT on Occult Lymph Node Metastasis for Patients with Clinical Stage IA-IIA Lung Adenocarcinoma: A Double-Center Study [J]. Acad Radiol, 2023, 30(12): 2870-2879.
[6] SUN Q, LI P, ZHANG J, et al. CT Predictors of Visceral Pleural Invasion in Patients with Non-Small Cell Lung Cancers 30 mm or Smaller [J]. Radiology, 2024, 310(1): e231611.
[7] ZHANG Y, SUN Y, XIANG J, et al. A clinicopathologic prediction model for postoperative recurrence in stage Ia non-small cell lung cancer [J]. J Thorac Cardiovasc Surg, 2014, 148(4): 1193-1199.
[8] KIM I H, LEE I H, LEE J E, et al. Prognostic Impact of Multiple Clinicopathologic Risk Factors and c-MET Overexpression in Patients Who Have Undergone Resection of Stage IB Non-Small-Cell Lung Cancer [J]. Clin Lung Cancer, 2016, 17(5): e31-e43.
[9] ZHANG N, TAN Q, TAO D, et al. Cytokines screening identifies MIG (CXCL9) for postoperative recurrence prediction in operated non-small cell lung cancer patients [J]. Cytokine, 2022, 149(155759).
[10] ARAK H, AYTEKIN A, CANOZ O, et al. Prognostic and Predictive Significance of PD-L1 Expression in Non-Small Cell Lung Cancer Patients: A Single-Center Experience [J]. Turk Patoloji Derg, 2021, 37(3): 239-248.
[11] WANG G, ZHAO M, LI J, et al. m7G-Associated subtypes, tumor microenvironment, and validation of prognostic signature in lung adenocarcinoma [J]. Front Genet, 2022, 13(954840).
[12] WU P, ZHENG Y, WANG Y, et al. Development and validation of a robust immune-related prognostic signature in early-stage lung adenocarcinoma [J]. J Transl Med, 2020, 18(1): 380.
[13] ZENG B, JI P, CHEN C, et al. A nomogram from the SEER database for predicting the prognosis of patients with non-small cell lung cancer [J]. Int J Biochem Cell Biol, 2020, 127(105825).
[14] LIU Y, HUANG C, LIU H, et al. Sublobectomy versus lobectomy for stage IA (T1a) non-small-cell lung cancer: a meta-analysis study [J]. World J Surg Oncol, 2014, 12(138).
[15] ZHANG X X, LI R, FAN L H, et al. Prognostic predictors of radical resection of stage I-IIIB non-small cell lung cancer: the role of preoperative CT texture features, conventional imaging features, and clinical features in a retrospectively analyzed [J]. BMC Pulmonary Medicine, 2023, 23 (1): 122.
[16] ZHANG Y, QIANG J W, YE J D, et al. High resolution CT in differentiating minimally invasive component in early lung adenocarcinoma [J]. Lung Cancer, 2014, 84(3): 236-41.
[17] SHIMIZU K, YAMADA K, SAITO H, et al. Surgically curable peripheral lung carcinoma: correlation of thin-section CT findings with histologic prognostic factors and survival [J]. Chest, 2005, 127(3): 871-8.